

Entanglement concentration of continuous variable quantum states

Jaromír Fiurášek, Ladislav Mišta, Jr., and Radim Filip
Department of Optics, Palacký University, 17. listopadu 50, 77200 Olomouc, Czech Republic

We propose two probabilistic entanglement concentration schemes for a single copy of two-mode squeezed vacuum state. The first scheme is based on the off-resonant interaction of a Rydberg atom with the cavity field while the second setup involves the cross Kerr interaction, auxiliary mode prepared in a strong coherent state and a homodyne detection. We show that the continuous-variable entanglement concentration allows us to improve the fidelity of teleportation of coherent states.

PACS numbers: 03.67.-a, 42.50.Dv

I. INTRODUCTION

Quantum entanglement is an essential ingredient of many protocols for quantum information processing such as quantum teleportation [1, 2] or quantum cryptography [3]. In order to achieve optimum performance of these protocols, the two involved parties, traditionally called Alice and Bob, should share a pure maximally entangled state. In practice, however, we are often able to generate only non-maximally entangled state and, in addition, the distribution of the entangled state between the two distant parties via some noisy quantum channel will degrade the entanglement and Alice and Bob will share some partially entangled mixed state. One of the most important discoveries in the quantum information theory was the development of the entanglement purification protocols that allow Alice and Bob to extract a small number of highly entangled almost pure states from a large number of weakly entangled mixed states [4, 5, 6]. These protocols involve only local operations and classical communication (LOCC) between the two parties, therefore they can be performed after the distribution of the entangled states.

In the simplest scenario Alice and Bob share a pure non-maximally entangled state in a d -dimensional Hilbert space whose Schmidt decomposition reads

$$|\psi\rangle = \sum_{j=1}^d c_j |\alpha_j\rangle_A |\beta_j\rangle_B, \quad (1)$$

where each set of states $|\alpha_j\rangle$ and $|\beta_j\rangle$ forms a basis. Alice and Bob would like to prepare from $|\psi\rangle$ a state with higher entanglement by means of LOCC operations. Remarkably, this is possible, albeit only with certain probability, even if they share only a single copy of this state. The procedure that accomplishes this task was fittingly called the Procrustean method [4], because it cuts off the Schmidt coefficients c_j to the size of the smallest one. In this way, Alice and Bob obtain, with certain probability, a maximally entangled state in a d -dimensional Hilbert space.

In view of the recent interest in quantum information processing with continuous variables [2, 7, 8, 9, 10], it is highly desirable to establish experimentally feasible entanglement distillation and concentration protocols for

the continuous variables. Of particular importance are the protocols for Gaussian states, because these states can be prepared in the lab with the use of commonly available resources comprising lasers, passive linear optics and squeezers (parametric amplifiers). However, it was proved recently that it is impossible to distill Gaussian entangled states by means of Gaussian operations only [11]. This means that additional resources beyond the linear optics and homodyne detectors are required. The distillation protocols for Gaussian states proposed so far employ the photon-number measurements. The scheme suggested by Duan *et al.* [12] relies on nondemolition measurement of the total photon number in two (or more) modes and represents a direct extension of the Schmidt projection method to infinite-dimensional Hilbert space. The Procrustean schemes considered by Opatrný *et al.* [13] and further analyzed by Cochrane *et al.* [14] are based on a controlled addition and subtraction of photons. We also note that several distillation schemes for entangled coherent states have been proposed [15, 16].

In this paper, we design two entanglement-concentration setups for a single copy of pure two-mode squeezed vacuum state

$$|\psi\rangle = \sum_{n=0}^{\infty} c_n |n, n\rangle, \quad c_n = \sqrt{1 - \lambda^2} \lambda^n, \quad (2)$$

where $\lambda = \tanh r$ and r is the squeezing constant. This state can be generated in the process of a non-degenerate spontaneous parametric downconversion and provides a common source of the continuous-variable entanglement in the experiments. The Procrustean procedures that we are proposing preserve the structure of the state (2) while the Schmidt coefficients c_n are transformed to new ones, $c_n \rightarrow d_n$. The first scheme is based on a dispersive interaction of a two-level atom with the microwave cavity field and the atomic-state detection. The second scheme utilizes a cross Kerr interaction, coherent states, homodyne measurements, and linear optics. The underlying mechanism of both these schemes is that a certain auxiliary system experiences a phase shift that depends on the number of photons in the Alice's mode of the shared state (2). We convert this phase modulation into amplitude modulation via interference, which allows us to

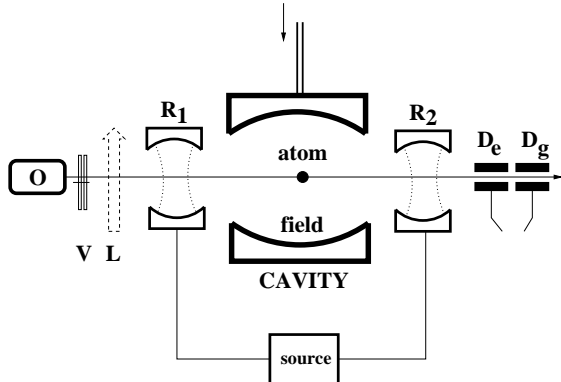


FIG. 1: Schematic of entanglement concentration setup in cavity QED: O is atomic oven, V is atomic velocity selector, L is laser excitation mechanism, R₁ and R₂ are the Ramsey zones driven by the microwave source, CAVITY contains the Alice's (Bob's) part of the entangled state and D_e, D_g are the field ionization detectors measuring the state of the Rydberg atom.

control the amplitude of the Schmidt coefficients c_n . An essential part of our probabilistic protocols is the measurement on the auxiliary system which tells us whether the concentration succeeded or failed.

The paper is organized as follows. The first scheme is analyzed in Sec. II and the second scheme is discussed in Sec. III. Finally, Sec. IV contains the conclusions.

II. ENTANGLEMENT CONCENTRATION IN CAVITY QED

Our first entanglement concentration scheme is designed for the quantum state of electromagnetic field confined in a high- Q cavity and is schematically sketched in Fig. 1. Note, that this setup has been successfully realized experimentally and employed for the QND measurements of the cavity-field photon number and the preparation of Schrödinger cat states [17, 18]. The scheme shown in Fig. 1 is based on an off-resonant interaction of an (effectively) two-level Rydberg atom with a single mode of a cavity sandwiched in the Ramsey interferometer. The atoms are emitted from an oven, their velocity is selected by the velocity selector, and are excited by a laser pulse to the upper level. Subsequently, each atom enters the first microwave Ramsey zone where it is prepared in a coherent superposition of the two (relevant) long-living circular Rydberg states $|g\rangle$ and $|e\rangle$,

$$|\phi\rangle = \frac{1}{\sqrt{2}}(|g\rangle + e^{i\varphi_0}|e\rangle). \quad (3)$$

The atom then traverses the cavity that contains the Alice's part of the shared two-mode state (2). The dispersive atom-field interaction in the cavity is governed by the following effective Hamiltonian

$$H = \hbar\kappa a^\dagger a \otimes |e\rangle\langle e|, \quad (4)$$

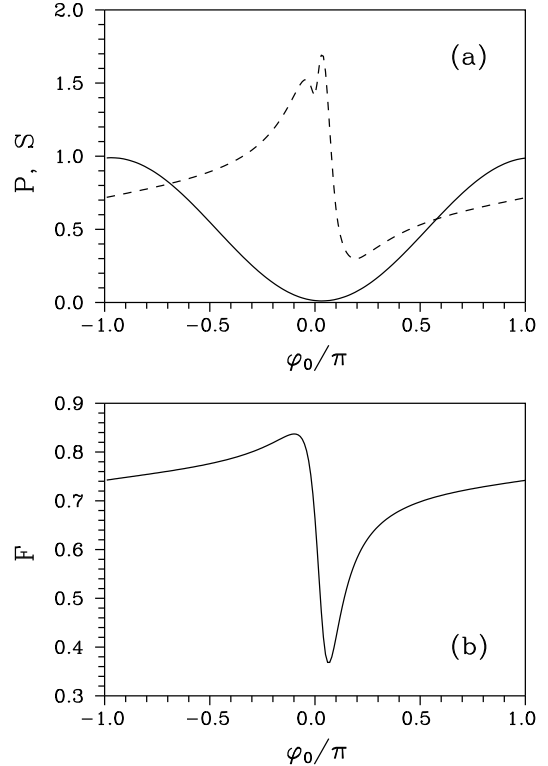


FIG. 2: The performance of the entanglement concentration scheme shown in Fig. 1 for $\lambda = 1/2$ and $\varphi = \pi/10$. (a) Probability of success P (solid line) and the von Neumann entropy S after the concentration (dashed line) and (b) the fidelity F of teleportation of coherent states are plotted as functions of φ_0 . For the input state, $S_{\text{in}} = 0.75$ and $F_{\text{in}} = 0.75$.

where a is annihilation operator of Alice's mode and κ is effective atom-field interaction constant. The coupling (4) results in a phase shift $\Delta\varphi = a^\dagger a \varphi$ of the state $|e\rangle$ that is linearly proportional to the number of photons in the mode A . On the other hand, the state $|g\rangle$ is not changed by the interaction. The single-photon phase shift $\varphi = \kappa t$, where t is an effective interaction time, can be adjusted to the required value by a proper selection of the atomic velocity.

After leaving the cavity, the atom passes through the second microwave Ramsey zone, where it undergoes a $\pi/2$ Rabi rotation,

$$|g\rangle \rightarrow \frac{1}{\sqrt{2}}(|g\rangle + |e\rangle), \quad |e\rangle \rightarrow \frac{1}{\sqrt{2}}(|e\rangle - |g\rangle). \quad (5)$$

The resulting state of the atom and the two-mode field reads

$$|\Psi\rangle = \frac{1}{2} \sum_{n=0}^{\infty} c_n (1 - e^{i\varphi_0 - in\varphi}) |g\rangle \otimes |n, n\rangle + \frac{1}{2} \sum_{n=0}^{\infty} c_n (1 + e^{i\varphi_0 - in\varphi}) |e\rangle \otimes |n, n\rangle. \quad (6)$$

To complete the procedure, we measure the state of the atom by means of state-selective ionization detectors exhibiting almost unit detection efficiency. The entanglement concentration succeeds only if the atom is found to be in the ground state $|g\rangle$. The new Schmidt coefficients after this conditional transformation read

$$d_n = i c_n \exp\left(i \frac{\varphi_0 - n\varphi}{2}\right) \sin\left(\frac{n\varphi - \varphi_0}{2}\right). \quad (7)$$

The irrelevant overall phase factor $i \exp(i\varphi_0/2)$ can be dropped. Moreover, the phase factor $\exp(-in\varphi/2)$ can easily be compensated by appropriate phase shift or simply by properly redefining the quadratures of the Alice's mode. After these transformations, the new Schmidt coefficients become real and after renormalization we get

$$d_n = \sqrt{\frac{1 - \lambda^2}{P}} \lambda^n \sin\left(\frac{n\varphi - \varphi_0}{2}\right), \quad (8)$$

where

$$P = \frac{1}{2} - \frac{1 - \lambda^2}{2} \frac{\cos(\varphi_0) - \lambda^2 \cos(\varphi + \varphi_0)}{1 - 2\lambda^2 \cos(\varphi) + \lambda^4} \quad (9)$$

is the probability of success of the conditional transformation. Clearly, two trends are competing in Eq. (8). The exponential decay λ^n is for certain n partially compensated by the second term $\sin[(n\varphi - \varphi_0)/2]$ which grows with n up to $n_{\max} = (\pi + \varphi_0)/\varphi$. This allows us to increase the entanglement of the shared state.

Formally, the conditional transformation can be described as a diagonal filter applied to the input two-mode density matrix ρ_{AB} . Define operator

$$A = \sum_{n=0}^{\infty} \sin\left(\frac{n\varphi - \varphi_0}{2}\right) |n\rangle\langle n|. \quad (10)$$

The output (unnormalized) density matrix is given by

$$\rho_{\text{out}} = A \otimes \mathbb{1}_B \rho_{ABA} A^\dagger \otimes \mathbb{1}_B, \quad (11)$$

where $\mathbb{1}_B$ stands for an identity operator on the Hilbert space of the Bob's mode.

Since the conditional transformation preserves the purity of the two-mode state, we can conveniently quantify the entanglement as the von Neumann entropy of the reduced density matrix of the Alice's mode,

$$S = - \sum_{n=0}^{\infty} |d_n|^2 \ln |d_n|^2. \quad (12)$$

The entropy S is plotted in Fig. 2(a) as a function of φ_0 for fixed φ and λ . Before concentration, Alice and Bob share two-mode squeezed vacuum (2), and the entropy (12) reads

$$S = -\ln(1 - \lambda^2) - \frac{\lambda^2}{1 - \lambda^2} \ln \lambda^2. \quad (13)$$

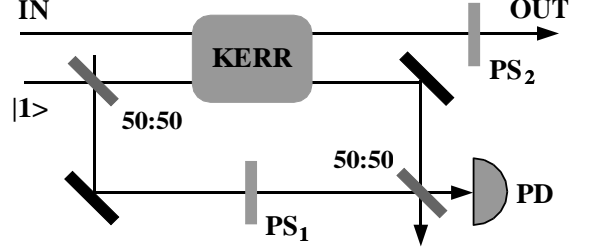


FIG. 3: Optical implementation of the entanglement concentration scheme shown in Fig. 1.

For the data in Fig. 2, we obtain $S_{\text{in}} = 0.75$. The figure 2(a) clearly shows that for certain interval of phase shifts φ_0 our procedure allows us to conditionally increase the amount of entanglement in the pure two-mode state shared by Alice and Bob.

Let us now demonstrate that the entanglement concentrated in this way is useful in practical tasks. To be specific, we consider the teleportation of coherent states in the Braunstein-Kimble scheme [2] where our state is used as the quantum channel. Making use of the transfer operator formalism [19, 20], we can express the fidelity of teleportation as follows,

$$F = \frac{1}{2} \sum_{m=0}^{\infty} \sum_{n=0}^{\infty} \binom{m+n}{n} \frac{d_m d_n^*}{2^{m+n}}. \quad (14)$$

On inserting the Schmidt coefficients (8) into Eq. (14) and carrying out the summations we obtain analytical formula for the fidelity of teleportation of coherent states,

$$F = \frac{1 - \lambda^2}{4P} \left[\frac{1}{1 - \lambda \cos(\varphi/2)} - \frac{\cos(\varphi_0) - \lambda \cos(\varphi/2 + \varphi_0)}{1 - 2\lambda \cos(\varphi/2) + \lambda^2} \right]. \quad (15)$$

The fidelity F is plotted in Fig. 2(b). For fixed λ and φ we can optimize the phase φ_0 so that the teleportation fidelity F will be maximized. For the data used in Fig. 2, we find that it is optimum to set $\varphi_0 \approx -\pi/10$, which yields the fidelity $F = 0.837$ and the probability of success is $P = 0.05$. This should be compared with the fidelity $F_{\text{in}} = 0.75$ that is achieved when the original two-mode squeezed vacuum with $\lambda = 1/2$ serves as the quantum channel. This improvement in fidelity is quite significant and clearly illustrates the practical utility of our procedure.

III. ENTANGLEMENT CONCENTRATION FOR TRAVELING LIGHT FIELDS

To implement the scheme discussed in the preceding Section for traveling light fields, we could replace the atomic Ramsey interferometer with a Mach-Zhender interferometer for a single photon and couple this auxiliary photon to the Alice's mode via nonlinear medium with cross Kerr effect, see Fig. 3. A similar setup has

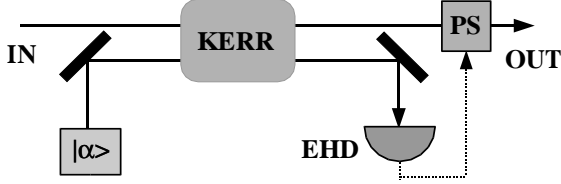


FIG. 4: Schematic of the entanglement concentration setup for traveling light fields that is based on auxiliary coherent states, cross Kerr interaction, eight-port homodyne detection (EHD), and a linear phase shift depending on the outcome of the measurement (PS).

been proposed by Gerry for the generation of Schrödinger cat states [21]. However, this scheme has several drawbacks. First, the currently achievable Kerr nonlinearities are rather low. Secondly, we have to prepare a single photon. Therefore we propose an alternative scheme, see Fig. 4. In that setup, an auxiliary mode C is prepared in a (strong) coherent state $|\alpha\rangle$ and then interacts with the Alice's mode A in the Kerr medium described by the Hamiltonian

$$H_{\text{Kerr}} = \hbar\kappa a^\dagger a c^\dagger c. \quad (16)$$

After the interaction, we project the output state into coherent state $|\beta\rangle$ in the eight-port homodyne detector.

The principle of the operation of this scheme may be explained as follows. If there are n photons in the mode A , then the coherent state $|\alpha\rangle$ evolves to $|\alpha e^{in\varphi}\rangle$, where $\varphi = -\kappa t$ and t is the effective interaction time. The probability of projecting into $|\beta\rangle$ is given by

$$P(\beta|n) = \frac{1}{\pi} |\langle \beta | \alpha e^{in\varphi} \rangle|^2. \quad (17)$$

From this formula we can see that the probability may grow with n if β belongs to certain region of the phase space. Without loss of generality, we may assume that α is real and positive and define $\beta = |\beta| \exp(i\varphi_0)$. After projecting into β , the new Schmidt coefficients can be expressed as

$$d_n \propto c_n \langle \beta | \alpha e^{in\varphi} \rangle. \quad (18)$$

Making use of the formula for the scalar product of two coherent states [22]

$$\langle \beta | \alpha \rangle = \exp \left(-\frac{1}{2} |\alpha|^2 - \frac{1}{2} |\beta|^2 + \beta^* \alpha \right) \quad (19)$$

we obtain

$$d_n \propto c_n \exp(q_n + i\phi_n), \quad (20)$$

where

$$q_n = |\alpha\beta| \cos(n\varphi - \varphi_0), \quad (21)$$

$$\phi_n = |\alpha\beta| \sin(n\varphi - \varphi_0). \quad (22)$$

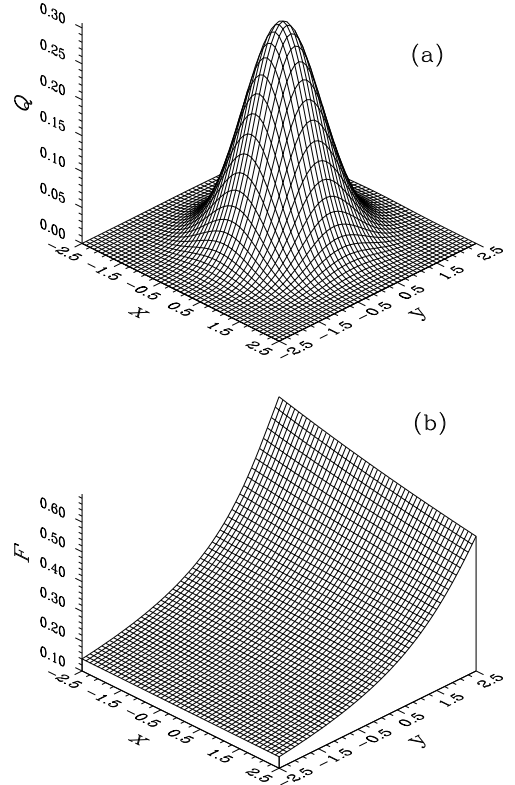


FIG. 5: (a) The Q-function $Q(\beta)$ of the output state of the auxiliary mode and (b) the overlap $F(\beta)$ are shown for $\lambda = 1/2$, $\alpha = 10$, $\varphi = \pi/100$, and $N = 10$. The coordinates x and y are defined as $x + iy = \beta - \alpha$.

The old coefficients c_n are amplified or de-amplified by the factor $\exp(q_n)$. The highest enhancement occurs for $n = \varphi_0/\varphi$, when $q_n = |\alpha\beta|$. For strong auxiliary signal $\alpha \gg 1$, the phase φ_0 between β and α will typically be of the order $|\varphi_0| \approx 1/|\alpha|$ and also $|\beta| \approx |\alpha|$ will hold. Since the nonlinear phase shift $n\varphi$ will typically be very small for all n for which c_n substantially differs from zero, $n\varphi \ll 1$, we can expand the expressions (21) and (22) in Taylor series and keep only terms up to linear in $n\varphi$,

$$\begin{aligned} q_n &= |\alpha\beta| \cos(\varphi_0) + n\varphi |\alpha\beta| \sin(\varphi_0), \\ \phi_n &= -|\alpha\beta| \sin(\varphi_0) + n\varphi |\alpha\beta| \cos(\varphi_0). \end{aligned} \quad (23)$$

This approximation is valid when

$$|\alpha|n\varphi \ll 1 \quad (24)$$

holds. Within this approximation the exponents q_n are linearly proportional to n and the conditional transformation preserves the structure of the two-mode squeezed state:

$$|d_n| \propto \tilde{\lambda}^n, \quad \tilde{\lambda} = \lambda \exp(\varphi |\alpha\beta| \sin \varphi_0). \quad (25)$$

Since $|\beta| \sin \varphi_0 \lesssim 1$, it is the product $\varphi |\alpha|$ that determines the modulation of the input Schmidt coefficients. A weak Kerr nonlinearity (small phase shift φ)

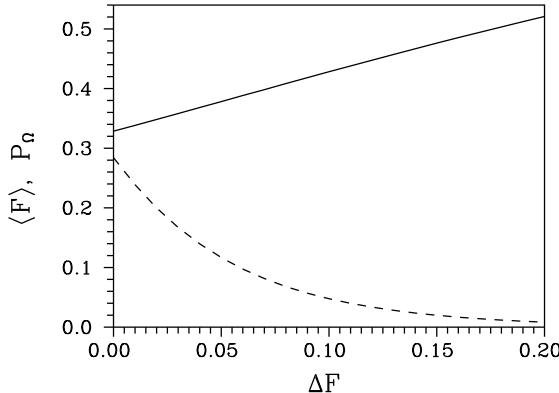


FIG. 6: The average fidelity $\langle F \rangle$ (solid line) and the probability of success (dashed line). All the parameters are the same as in Fig. 5.

can be compensated by using a sufficiently strong auxiliary coherent state $|\alpha\rangle$. Furthermore, the strength of the cross-Kerr interaction can be enhanced by many orders of magnitude in a coherently prepared resonant atomic medium. A medium with electromagnetically induced transparency can exhibit an extremely large Kerr nonlinearity [23, 24, 25, 26, 27] that would suffice for the practical implementation of the present entanglement concentration scheme.

One undesirable effect of the projection into coherent state $|\beta\rangle$ is the phase modulation ϕ_n of the Schmidt coefficients. Note, however, that if the approximation (24) holds then it follows from Eq. (23) that the conditional phase shift ϕ_n is linearly proportional to n and can thus be removed by a suitable phase shifter PS. The actual phase shift is proportional to the real part of β and we must use a feedforward scheme, where the operation of the PS (e.g., a Pockels cell) is controlled by the measurement outcome, as is schematically indicated in Fig. 4.

After this qualitative discussion, let us now provide a rigorous mathematical description of the entanglement concentration scheme shown in Fig. 4. The probability that β will be measured in the EHD is the sum of all the conditional probabilities $P(\beta|n)$ multiplied by the probabilities $|c_n|^2$ that there are n photons in the mode A ,

$$Q(\beta) = \frac{1 - \lambda^2}{\pi} \sum_{n=0}^{\infty} \lambda^{2n} \exp(-|\alpha e^{in\varphi} - \beta|^2). \quad (26)$$

The normalized Schmidt coefficients corresponding to the measurement outcome β read

$$d_n(\beta) = \frac{\sqrt{1 - \lambda^2} \lambda^n \exp[\alpha \beta^* e^{in\varphi} - in\varphi |\alpha \beta| \cos \varphi_0]}{\sqrt{\pi Q(\beta)} \exp(|\alpha|^2/2 + |\beta|^2/2)}. \quad (27)$$

We need to establish a criterion according to which we will accept or reject the state in dependence on the measurement outcome β . The most natural approach is to

choose some reasonable figure of merit $\mathcal{F}(\beta)$ that has to be evaluated for each β and then specify a region Ω in the phase space where this figure of merit is sufficiently large. The entanglement concentration succeeds only if $\beta \in \Omega$ and fails otherwise. It follows that the concentration will yield a mixture of the states

$$|\psi(\beta)\rangle = \sum_{d=0}^{\infty} d_n(\beta) |n, n\rangle \quad (28)$$

and the density matrix of the output state shared by Alice and Bob can be expressed as follows,

$$\rho_{\Omega} = \frac{1}{P_{\Omega}} \int_{\Omega} d^2\beta Q(\beta) |\psi(\beta)\rangle \langle \psi(\beta)|. \quad (29)$$

Here

$$P_{\Omega} = \int_{\Omega} d^2\beta Q(\beta) \quad (30)$$

denotes the probability of success of the concentration, i.e., the probability that the measurement outcome β will belong to Ω .

Different figures of merit $\mathcal{F}(\beta)$ may be suitable depending on the intended usage of the shared quantum state. For instance, if that state shall be used to teleport coherent states, then it will be natural to employ the fidelity (14) as the figure of merit. Here we make use of an even simpler quantity, namely the fidelity

$$\mathcal{F}(\beta) = |\langle \Phi_N | \psi(\beta) \rangle|^2 \quad (31)$$

between the conditionally prepared state and a maximally entangled state in the Hilbert space of the first $N + 1$ Fock states,

$$|\Phi_N\rangle = \frac{1}{\sqrt{N+1}} \sum_{n=0}^N |n, n\rangle, \quad (32)$$

The fidelity depends on the sum of the first $N+1$ Schmidt coefficients and is explicitly given by the following formula,

$$\mathcal{F}(\beta) = \frac{1}{N+1} \left| \sum_{n=0}^N d_n(\beta) \right|^2. \quad (33)$$

In the rest of this section we present the results of the numerical calculations for $\alpha = 10$, $\varphi = \pi/100$, and $\lambda = 1/2$. The Q -function (26) of the output auxiliary mode is plotted in Fig. 5(a). Since the assumed nonlinear single-photon phase shift $\pi/100$ is relatively small, the Q -function is practically identical to the input Gaussian $Q_{\text{in}}(\beta) = \exp(-|\alpha - \beta|^2)/\pi$. The function $\mathcal{F}(\beta)$ is plotted in Fig. 5(b) for $N = 10$. We can see that there are regions in the phase space where \mathcal{F} is higher than the fidelity corresponding to the input two-mode squeezed vacuum, $\mathcal{F}_0 = 0.273$. As described above, we define Ω as

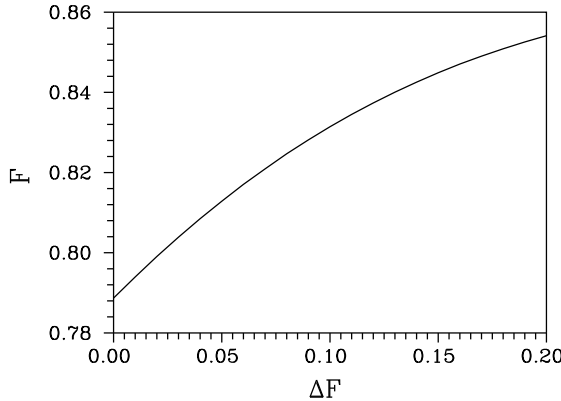


FIG. 7: The fidelity of the teleportation of coherent states when the state ρ_Ω after concentration is used as the quantum channel. All parameters are the same as in Fig. 5.

the region of the phase space where $\mathcal{F}(\beta) \geq \mathcal{F}_0 + \Delta\mathcal{F}$. The dependence of the average fidelity

$$\langle \mathcal{F} \rangle = \frac{1}{P_\Omega} \int_\Omega d^2\beta Q(\beta) \mathcal{F}(\beta) \quad (34)$$

on $\Delta\mathcal{F}$ is plotted in Fig. 6. Also the probability of successful entanglement concentration (30) is shown there. As the gap $\Delta\mathcal{F}$ becomes larger, the average fidelity increases while the probability decreases.

Finally, we show that the entanglement concentrated in this way is suitable for the teleportation. We can calculate the average teleportation fidelity similarly as $\langle \mathcal{F} \rangle$. We evaluate the fidelity of teleportation $F(\beta)$ for each $\beta \in \Omega$ by inserting the relevant Schmidt coefficients $d(\beta)$ given by Eq. (27) into Eq. (14) and then we average $F(\beta)$ over Ω with the properly normalized probability density

$Q(\beta)/P_\Omega$. The results are shown in Fig. 7. We can see that the teleportation fidelity monotonically grows with $\Delta\mathcal{F}$ and for all $\Delta\mathcal{F} > 0$ we have $F > 0.75$. This example confirms that our procedure indeed extracts more useful entanglement from the input two-mode squeezed vacuum.

IV. CONCLUSIONS

In this paper, we have designed two schemes for probabilistic concentration of continuous-variable entanglement. The Procrustean protocols that we are proposing have the important property that they can be applied several times to a single copy of the shared two-mode entangled state. Thus we could, in principle, extract a state with very high entanglement, at the expense of a low probability of success. When repeating the concentration procedure, one could optimize the relevant parameters such as the phase shifts φ_0 and φ in order to achieve the optimum performance of the schemes. In view of the recent advances in cavity-QED experiments and the preparation of media with extremely high Kerr nonlinearity, we may hope that the schemes proposed in the present paper will become experimentally feasible in a near future.

Acknowledgments

This work was supported by the EU grant under QIPC project IST-1999-13071 (QUICOV) and project LN00A015 of the Czech Ministry of Education.

[1] C.H. Bennett, G. Brassard, C. Crepeau, R. Jozsa, A. Peres, and W.K. Wootters, Phys. Rev. Lett. **70**, 1895 (1993).

[2] L. Vaidman, Phys. Rev. A **49**, 1473 (1994); S.L. Braunstein and H.J. Kimble, Phys. Rev. Lett. **80**, 869 (1998); A. Furusawa, J.L. Sørensen, S.L. Braunstein, C.A. Fuchs, H.J. Kimble, and E.S. Polzik, Science **282**, 706 (1998); T.C. Ralph and P.K. Lam, Phys. Rev. Lett. **81**, 5668 (1998).

[3] A.K. Ekert, Phys. Rev. Lett. **67**, 661 (1991).

[4] C.H. Bennett, H.J. Bernstein, S. Popescu, and B. Schumacher, Phys. Rev. A **53**, 2046 (1996).

[5] C.H. Bennett, G. Brassard, S. Popescu, B. Schumacher, J.A. Smolin, and W.K. Wootters, Phys. Rev. Lett. **76**, 722 (1996).

[6] D. Deutsch, A. Ekert, R. Jozsa, C. Macchiavello, S. Popescu, and A. Sanpera, Phys. Rev. Lett. **77**, 2818 (1996).

[7] G. Lindblad, J. Phys. A: Math. Gen. **33**, 5059 (2000); N.J. Cerf, A. Ipe, and X. Rottenberg, Phys. Rev. Lett. **85**, 1754 (2000); J. Fiurášek, Phys. Rev. Lett. **86**, 4942 (2001); S.L. Braunstein, N.J. Cerf, S. Iblisdir, P. van Loock, and S. Massar, Phys. Rev. Lett. **86**, 4938 (2001).

[8] S.L. Braunstein, Phys. Rev. Lett. **80**, 4084 (1998). Nature (London) **394**, 47 (1998); S. Lloyd and J.J.E. Slotine, Phys. Rev. Lett. **80**, 4088 (1998).

[9] T.C. Ralph, Phys. Rev. A **61**, 010303(R) (2000); M. Hillery, Phys. Rev. A **61**, 022309 (2000); N.J. Cerf, M. Levy, G. Van Assche, Phys. Rev. A **63**, 052311 (2001); F. Grosshans and P. Grangier, Phys. Rev. Lett. **88**, 057902 (2002); Ch. Silberhorn *et al.*, Phys. Rev. Lett. **88**, 167902 (2002).

[10] P. van Loock and S.L. Braunstein, Phys. Rev. A **61**, 010302(R) (1999); S.M. Tan, Phys. Rev. A **60**, 2752 (1999).

[11] J. Eisert, S. Scheel, and M.B. Plenio, quant-ph/0204052; J. Fiurášek, quant-ph/0204069, G. Giedke and J.I. Cirac, quant-ph/0204085.

[12] L.M. Duan, G. Giedke, J.I. Cirac, and P. Zoller, Phys. Rev. Lett. **84**, 4002 (2000); Phys. Rev. A **62**, 032304 (2000).

[13] T. Opatrný, G. Kurizki, and D.-G. Welsch, Phys. Rev.

A **61**, 032302 (2000).

[14] P.T. Cochrane, T.C. Ralph, and G.J. Milburn, quant-ph/0108051.

[15] S. Parker, S. Bose, and M.B. Plenio, Phys. Rev. A **61**, 032305 (2000).

[16] J. Clausen, L. Knöll, and D.-G. Welsch, quant-ph/0203144.

[17] M. Brune, S. Haroche, J.M. Raimond, L. Davidovich, and N. Zagury, Phys. Rev. A **45**, 5193 (1992).

[18] M. Brune, E. Hagley, J. Dreyer, X. Maitre, A. Maali, C. Wunderlich, J. M. Raimond, and S. Haroche, Phys. Rev. Lett. **77**, 4887 (1996).

[19] H.F. Hofmann, T. Ide, T. Kobayashi, and A. Furusawa, Phys. Rev. A **62**, 062304 (2000).

[20] S.I.J. Kurzeja and A.S. Parkins, quant-ph/0201094.

[21] C. Gerry, Phys. Rev. A **59**, 4095 (1999).

[22] J. Peřina, *Quantum Statistics of Linear and Nonlinear Optical Phenomena* (Kluwer: Dordrecht, 1991).

[23] H. Schmidt and A. Imamoglu, Opt. Lett. **21**, 1936 (1996).

[24] A. Imamoglu, H. Schmidt, G. Woods, and M. Deutsch, Phys. Rev. Lett. **79**, 1467 (1997).

[25] L.V. Hau, S.E. Harris, Z. Dutton, and C.H. Behroozi, Nature (London) **397**, 594 (1999).

[26] M.M. Kash *et al.*, Phys. Rev. Lett. **82**, 5229 (1999).

[27] M.D. Lukin and A. Imamoglu, Phys. Rev. Lett. **84**, 1419 (2000).